Modeling And Mapping Water Erosion Risks In The High Atlas Of Morocco: The Atlas Of Beni Mellal As A Case In Point

M. Bachaoui, B. Bachaoui, R. Lhissou, A. El harti et A. El GHmari

Sultan Moulay Slimane University, Faculty of Sciences and Techniques of Beni Mellal,
Team of Remote Sensing and GIS Applied to the Geosciences and the Environment, -Morocco-

KEYWORDS: Water erosion, remote sensing, spectral indices, multi-criteria analysis, High atlas, Morocco.

ABSTRACT

The aim of this work is to show the importance of the use of remote sensing and Geographic Information Systems (GIS) to map soil degradation by water erosion in the Atlas of Beni Mellal located in Moroccan central High Atlas. To reach this goal, we have followed a methodology based, on the one hand, on the Spectral Indices approach (SI, BI and NDVI) and on the Spectral Angle Mapper (SAM) and Spectral Information Divergence (SID) supervised classifications, and, on the one hand, on a multi-criteria analysis (MCA) of the various factors involved in water erosion (slope, friability, and land use). The water erosion risk maps obtained were compared to ground truth for validation.

INTRODUCTION

Land degradation in Morocco is mainly due to water erosion whose effects have impacts on both water and soil potentials. The damages consist in the reduction of the area of agricultural lands (Merzouk et al., 1994), desertification of natural environment, an accelerated rate of siltation of reservoirs, thus reducing the quality and quantity of available waters, and the reduction in the lifetime of dams. According to Merzouk (1992), the large dams in Morocco receive about 50 million tons of sediment per year, which reduces the water storage capacity to about 0.5% per year (Tahri et al., 1993).

The central High Atlas that was in the past covered by vast forest areas (Leveque, 1961) is currently experiencing a continuing degradation due to drought and unmeasured exploitation. In this way, forest clearance has been done for the sake of using wood as fuel and as building material, for creating spaces for culture, for grazing, etc. This intensive situation of the land ground has led to the

destruction of vegetation and has exposed soil to erosive actions that have caused various damages.
The study area, which is part of the Moroccan central High Atlas, has rugged terrains and irregular rainfall patterns characterized by alternating periods of drought and very erosive torrential rains, less permeable soils, discontinuous vegetation that is sensitive to gullying, and a forest that is affected by deforestation by humans.

This situation results in floodings that cause a lot of damage. The sediment load carried by the wadis that cross the city of Beni Mellal cause serious damage to the infrastructure and also to the cleanliness of the city, in spite of the efforts made in the development of riverbeds and of sewerage.

PRESENTATION OF STUDY AREA

The study zone is situated in the western part of the central High Atlas, between altitudes 32° 17'N and 32° 24'N and longitudes 6° 14'W and 6° 23'W at an altitude varying between 600 and 2000m (***Fig. 1***).

The geology of the region is dominated by limestone formations of the Jurassic age. They are constituted by dolomites, bedded limestone and marls, covered in places by Quaternary terraces. The climate is of a continental type. This site is located in mountainous areas and is marked by a great irregularity in the amounts of precipitation and a regression of vegetation cover due to human action.

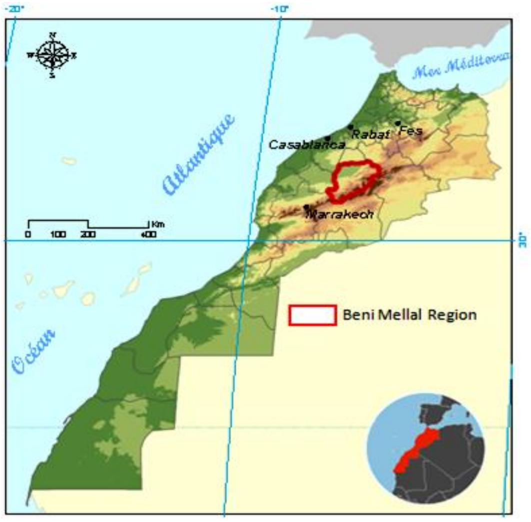

Figure 1: Geographical location of the Atlas of Beni Mellal

METHODOLOGY AND DATA USED

The methodology followed in this research is illustrated in ***Figure 2*** (annexed in the end of paper). It is divided into four main steps: i) The first relates to corrections of radiometric anomalies specific to the sensor and atmosphere effects, as well as to the geometric corrections, ii) The second step is based on the calculation of spectral indices (coloration index CI, shape index SI, Brightness Index BI and Normalized Difference Vegetation Index, NDVI), principal component analysis PCA, multi-criteria analysis MCA and supervised classifications SID and SAM°, iii) The third step is the derivation of topographic attributes (the gradient and the form of the slope) and the friability of soils, iv) And finally, the fourth step is the integration of all these parameters in a GIS environment according to a multi-criteria analysis for mapping of areas that are degraded or exposed to water erosion risks.

1. Cartographic Data

The topographic and geological maps were used for the extraction of information from the study area. We have used these maps as a database for the scanning and digitizing of contours and geological layers limits. Digitizing was performed after having georeferenced maps according to Lambert projection North Morocco. These maps have allowed us to develop a digital elevation model of (DEM), the slope, and the soil friability. Digitization has affected all contours of the study site in order to ensure that the DEM is closer to reality.

2. Field observations

Observations were made on about thirty sites well distributed over the study area and covering the different states of erosion in order to validate the results. The parameters observed were: slope, soil friability, vegetation cover, organic matter, texture and structure of soils.

3. Satellite images

The Aster Satellite image used was acquired on 28 July 2000. Aster sensor covers a wide spectral region with 14 bands covering the visible, shortwave infrared and thermal infrared. The spatial resolution varies with wavelength: 15 m in the visible and near infrared (VNIR), 30 m in the shortwave infrared (SWIR) and 90 m at thermal infrared (TIR). Once the satellite image was subject to atmospheric and geometric corrections, we performed the extraction of the different factors that were involved in the process of water erosion. Images of very high spatial resolution (2.5 m) of the Geo-Eye Google Earth sensor were then used to validate the obtained results.

RESULTS

1. Distinction of degraded areas using spectral indices and PCA

1.1. Color Index (CI)

Color is an environment parameter that characterizes the state of the soil. Thus, the spectral signature of the soil varies according to several parameters, such as organic matter content, moisture rate and mineralogical composition content. These variables have an important impact on the color and brightness of a soil (Bannari et al, 1996). Erosion processes can damage the surface horizon, which is rich in organic matter that makes the soil clearer and brighter. The calculation of the color Index (CI) is made from bands of the visible channels (bands 1 and 2) as proposed by Escadafal and *al*. (1994) (Equation .1). The slightly degraded soils are associated with low values of CI, much degraded soils are characterized by higher values of CI, and moderately degraded soils have intermediate values.

$$CI = \frac{\rho_2 - \rho_1}{\rho_2} \quad (1)$$

ρ_1, Measured reflectance at the green band ASTER 1;
ρ_1, Measured reflectance at the red band ASTER 2.

1.2. Shape Index (SI)

The reflectance curve shape of a soil is determined by the reflectance and absorption properties of the components of this soil. These properties can be used to detect the main components of the soil, especially organic matter, iron oxides, clay minerals and carbonates whose presence is an index of soil development. SI index is calculated from the red band and short wave infrared bands (Equation 2). Bands 6 and 8 correspond to peaks of clays and limestone absorption, which are considered as indirect indices of land degradation (Maimouni et al, 2011; Mathieu et al, 2007; Haboudane et al, 2002). The obtained results show that the highly degraded soils are associated with low values of SI whereas low degraded soils are characterized by higher values.

$$\mathrm{SI} = \frac{2\rho_8 - \rho_6 - \rho_2}{\rho_6 - \rho_2} \qquad (2)$$

ρ_2, Measured reflectance at the red band ASTER 2;
ρ_6, Measured reflectance at the SWIR band ASTER 6;
ρ_8, Measured reflectance at the SWIR band ASTER 6.

1.3. Normalized Difference Vegetation Index (NDVI)

The erosion risks increases when the vegetation cover is weak. The vegetation protects the soil from the impact of raindrops, tends to slow the rate of water runoff and, consequently, allows a better infiltration. The vegetation cover improves soils' cohesion and, in this way, it strengthens their mechanical properties. For the quantification of the vegetation cover, several vegetation indices have been developed. The most popular and widely used is the normalized difference index (*Normalized Difference Vegetation Index*, or NDVI) developed by Rouse *et al.* in 1974. The concept of NDVI development is based on the input of channels of red and near-infrared because these ones contain about 90% of the spectral information on the living vegetation (Baret *et al.* 1988). The NDVI is determined by the following formula.

$$\frac{\rho_3 - \rho_2}{\rho_3 + \rho_2} \qquad (3)$$

ρ_2, Measured reflectance at the red band ASTER 2;
ρ_3, Measured reflectance at the NIR band ASTER 3.

1.4. Brightness Index (BI)

The brightness of a soil can be an indicator of the state of degradation. A leached soil too tends to be brighter than organic-rich soil. The BI calculated from the visible bands (1 and 2) differentiates between levels of degradation. Thus, highly degraded soils have a relatively high BI, while developed soil are characterized by low values of BI.

The combination of the spectral indices SI, BI, CI, NDVI and the principal component analysis (PCA) allowed to discriminate between classes of soil degradation. Several combinations of colored compositions are tested. The combination between the CI, the SI and the principal component PC-2 has identified the vegetation classes and the state of soil degradation as shown in the ***Figure 3*** bellow.

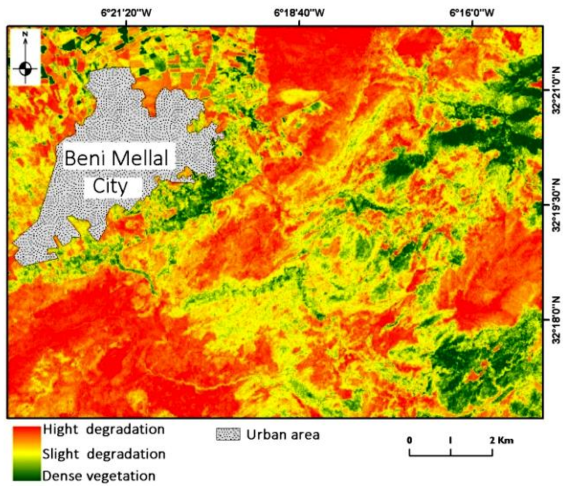

Figure 3: Map produced using the spectral indices and PC2 combination

2. Identification of soil degradation by SAM and SID Supervised Classifications

SAM (Spectral Angle Mapper) is a supervised classification based on the comparison between prototype spectral signatures (endmembers) that characterize each class of degradation and the evaluated pixels. That is, the smaller the spectral angle "α" is, the larger is the similarity between the spectrum of the evaluated pixel and the endmembers signature (Kruse et al., 1993; Cròsta et al., 1998). In our case, the best obtained result is an angle of 0.12 radians which permitted to identify four soil classes and two vegetation classes ***(Fig. 4)***.
SID classification is made by using the same endmembers used on SAM. SID requires a 'Maximum Divergence Threshold' parameter. This is, in fact, the minimum permissible variation distance between the spectral vector of the endmember and the pixel vector. The 0.05 default value can vary significantly according to regions.

Five threshold values from 0.05 to 0.09 were tested. A setting with a unique value of 0.08 was maintained for all endmembers because it provides better accuracy. The resulting map is shown in the ***Figure 5***. The results are slightly similar to those obtained by SAM classification. Sparse vegetation represents 34% of the area against 31% obtained by SAM classification.

The areas of strongly and heavily degraded soils are estimated at 29% and 30% respectively obtained by SID and SAM classifications. However, the two classifications have shown relatively different areas for slightly and moderately degraded soils.

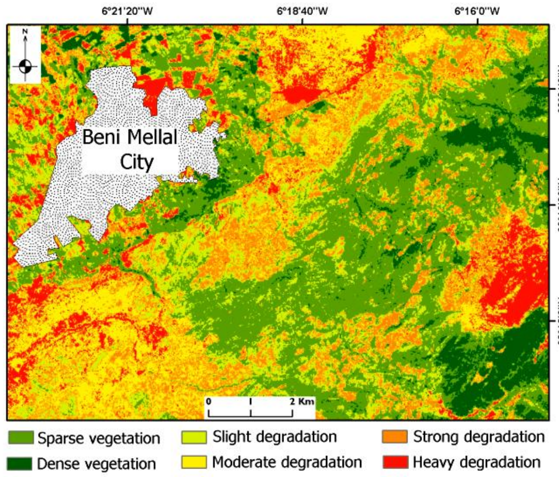

Figure 4: The ASTER imagery classification using the SAM technique

Land Occupation	index assigned
dense vegetation	1
sparse vegetation	2
cultivated land	3
bare land	4

Table 1: Soil occupation and indices assigned

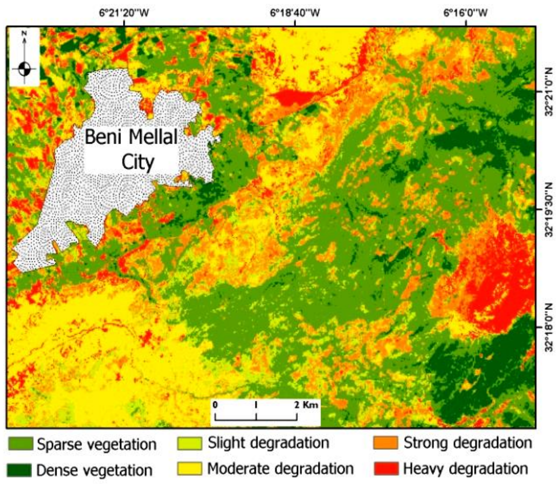

Figure 5: The ASTER imagery classification using the SID technique

3. Land use

Supervised classification of the ASTER Image has allowed to produce a land use map. According to our knowledge and field observations, five major classes were selected: cultivated land, bare land, dense vegetation, sparse vegetation and the urban area (***Fig. 6***).

At each class is assigned a value between 1 and 4: 1 being assigned to the least vulnerable class and 4 to the most vulnerable class (***Tab. 1***).

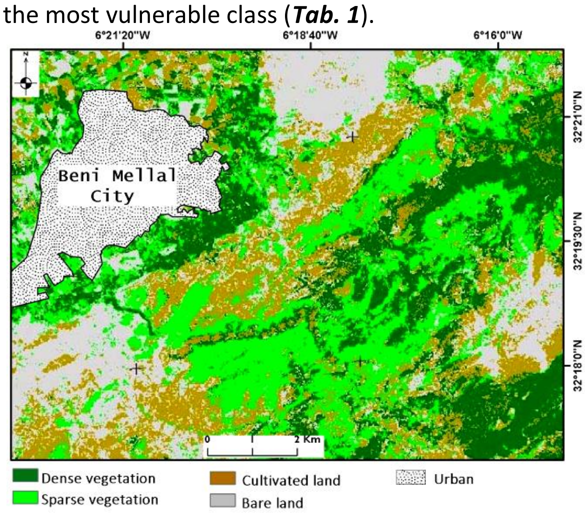

Figure 6: Map of land use

4. Cartography of soil erosion by multi-criteria analysis (MCA)

The MNA generated from the topographic map was used to produce the slope map. Four slope classes are distinguished: (0 - 5°, 5- 15°, 15-35° and 35-90°). Each class of slope is assigned an index varying from 1 to 4 (***Tab. 2***): one being assigned to low slopes (< 5°) and 4 to steep slopes (> 35°). These slope classes are defined on the basis of field observations of the state of erosion during the rainy season.

Slope classes in degree	Assigned index
0-5	1
5-15	2
15-35	3
35-90	4

Table 2: Indices assigned to the slope classes

Based on their sensitivity to erosion, erosion classes are normalized in a range of values from 1 to 4: 1 represents the low level of sensitivity to erosion and 4 indicates the highest level of sensitivity to erosion. These data are integrated into a GIS for a better management of information. The combination of the slope layer and the land use layer, following the decision rule mentioned in ***Table 3***, has allowed to obtain an erosion potential map.

Then final erosion map (***Fig. 7***) was developed by the interaction between the erosion potential map obtained in the previous step and the friability of materials obtained with the help of the decision rule presented in ***Table 4***. The final map comprises four classes: low degraded soil, moderately degraded soil, highly degraded soil, and greatly degraded soil.

Erosion Risk		**Slope degree**			
		1	**2**	**3**	**4**
Land use	**1**	1	2	3	3
	2	1	2	3	3
	3	2	3	3	4
	4	2	4	4	4

Table 3: Decision rule according to the slope

Erosion Risk		**Materials friability**			
		1	**2**	**3**	**4**
Erosion potential	**1**	1	1	1	2
	2	1	1	2	3
	3	2	2	4	4
	4	3	4	4	4

Table 4 : Decision rule according to the materials friability

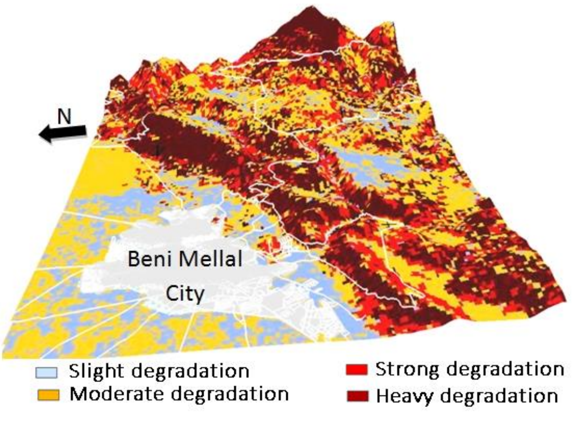

Figure 7: 3D Map of soil degradation resulting by multicriteria analyzes (MCA)

VALIDATION OF RESULTS

About thirty samples well distributed over the different obtained classes of erosion, with GeoEye-2 spatial high resolution images, MNA and field photographs and observations were used as validation tools for our results (***Figure 8 and Figure 9 annexed below***). ***Figure 9*** illustrates the validation of maps by the Geo-Eye 2 imaging. Validation was also made by the direct confrontation with the field reality by calculating the confusion matrix between the obtained classes and the field data.

For the SID, the overall accuracy and Kappa coefficient are 88% and 85% respectively. As to SAM classification, the overall accuracy and kappa coefficient are 75% and 70% respectively. The MAC and the spectral indices approach recorded an overall accuracy of 80% and 71% respectively and a Kappa coefficient of 75% and 66% respectively.

Confusion matrices also showed that the SID presents a slight confusion between low and moderately degraded soils against the SAM, MCA and spectral indices that showed confusion between the moderately, highly and greatly degraded classes. Validation by spatial high resolution image shows that the thematic classes were precisely mapped and perfectly coincided with the field reality (***Fig. 9***). The six thematic classes conducted are mapped similarly to the field reality while taking into account the relief.

Degraded soils are concentrated in the foothills and in high mountains. Soils with important slopes and deprived of vegetation are greatly degraded and are exposed to water erosion (**Fig**. 8)

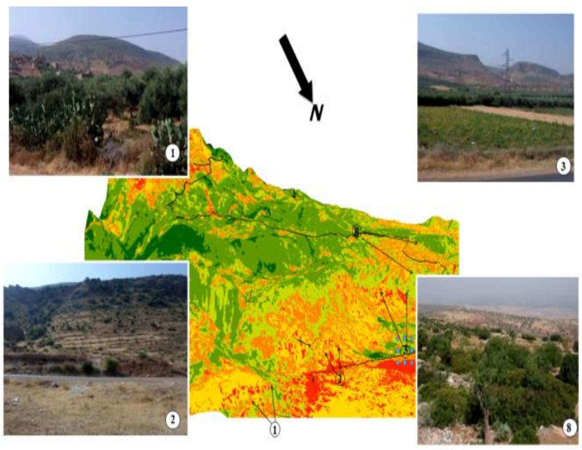

classifications SAM and SID by GeoEye image and by field observations

CONCLUSION

During this work, which consists of mapping degraded areas and areas exposed to water erosion in the vicinity of Beni Mellal area in the Moroccan central High Atlas, we have tested three approaches: (1) An approach based on spectral indices CI, SI, BI, NDVI and PCA; (2) An approach of supervised classifications: Spectral Information Divergence (SID) and Spectral Angle Mapper (SAM; (3) A Multi-Criteria Analysis (MCA) approach that integrates geomorphic variables such as slope inclination, land friability, and land occupation. The results thus obtained were assessed and exposed to ground truth for each method. This has provided slightly varying results, broadly similar and conclusive.

REFERENCES

Bannari, A., Huete, A.R., Morin, D., et Zagolski, F., Effets de la couleur et de la brillance des sols sur les indices de végétation. *International Journal of Remote Sensing, Vol. 17, no 10, p. 1885_1906. doi: 10.1080/01431169608948745, 1996.*

Baret F., Guyot G., Begue A. et Maurel P. (). Complemenîary of middle-infiared with visible and near-inhed reflectance for monitoring wheat canopies. *Remote Sensing of Environment, vol. 26, p. 213-225, 1988*

Crosta, A.P., Sabine, C. and Taranik, J.V., Hydrothermal Alteration Mapping at Bodie, California, using AVIRIS Hyperspectral data. *Remote Sensing of Environment, vol. 65, n°. 3, p. 309-319, 1998.*

Escadafal, R., Belghit A. et Ben-Moussa A., Indices spectraux pour la télédétection de la dégradation des milieux naturels en Tunisie aride. *Actes du 6eme Symposium international sur les mesures physiques et signatures en télédétection, Val d'Isère (France), 17-24 janvier 1994, ISPRS-CNES, p. 253-259, 1994*.

Haboudane D, Bonn F., Royer A., Sommer S., Mehl W. (). Land Degradation and Erosion risk Mapping by Fusion of Spectrally Based Information and Digital Geomorphometric Attributes. *International Journal of Remote Sensing, vol. 18, 3795-3820*, *2002.*

Kruse, F.A., Lefkoff, A.B., Boardman, J.W., Heidebrecht, K.B., Shapiro, A.T., Barloon, P.J. et Goetz, A.F.H.,The spectral image processing system (SIPS) – interactive visualization and analysis of imaging spectrometer data. *Remote Sensing of Environment 44 (2–3), 145–163, 1993*.

Levêque, P., Contribution à l'étude géologique et hydrogéologique de l'Atlas de Demnate. Faculté des sciences de Bordeaux. Thèse *Doctorat, 366 p., 1961*

Maimouni, S., Bannari, A., El-Harti, A. et El-Ghmari, A., Potentiels et Limites des Indices Spectraux pour Caractériser la dégradation des Sols en Milieu Semi-aride. *Journal Canadien de Télédétection, Vol. 37, No, 3, p. 285-301, 2011*.

Mathieu, R., Cervelle, B., Rémy, D. et Pouget, M., Field-based and spectral indicators for soil erosion mapping in semi-arid Mediterranean environments (Coastal Cordillera of central Chile). *Earth Surface Processes and Land Forms, vol. 32, p. 13-31,* 2007.

Merzouki, A., Diagnostic de l'envasement des grands barrages marocains. *La Revue Marocaine du Génie Civil, vol., 38, p. 46-50, 1992.*

Merzouk A. Rayan J., Kacemi M, A perspective on soil erosion in Morroco's dry land semi-aride zone. *Acte du colloque international des sciences du sol : « Science du sol au développement », Rabat, Maroc, 6-8 Avril 1993. 12p*.

Rouse, J.W., Haas, R.W., Schell, J.A., Deering, D. W. et Harlan J.C. (). Monitoring the vernal advancement and retrogradation (Greenwave effect) of natural vegetation. *NASAJGSFCT Type III*, *final Report, Greenbelt, MD, USA, 1974.*

Tahiri, M., Merzouki A., Lamb, H.F et Maxted, R.W, Etude de l'érosion hydrique dans le plateau d'Imilchil dans le Haut-Atlas central - Utilisation d'un SIG. *Géo-Observateur, Rabat, Maroc, n°.3, p.51-60, 1993.*

ANNEXES

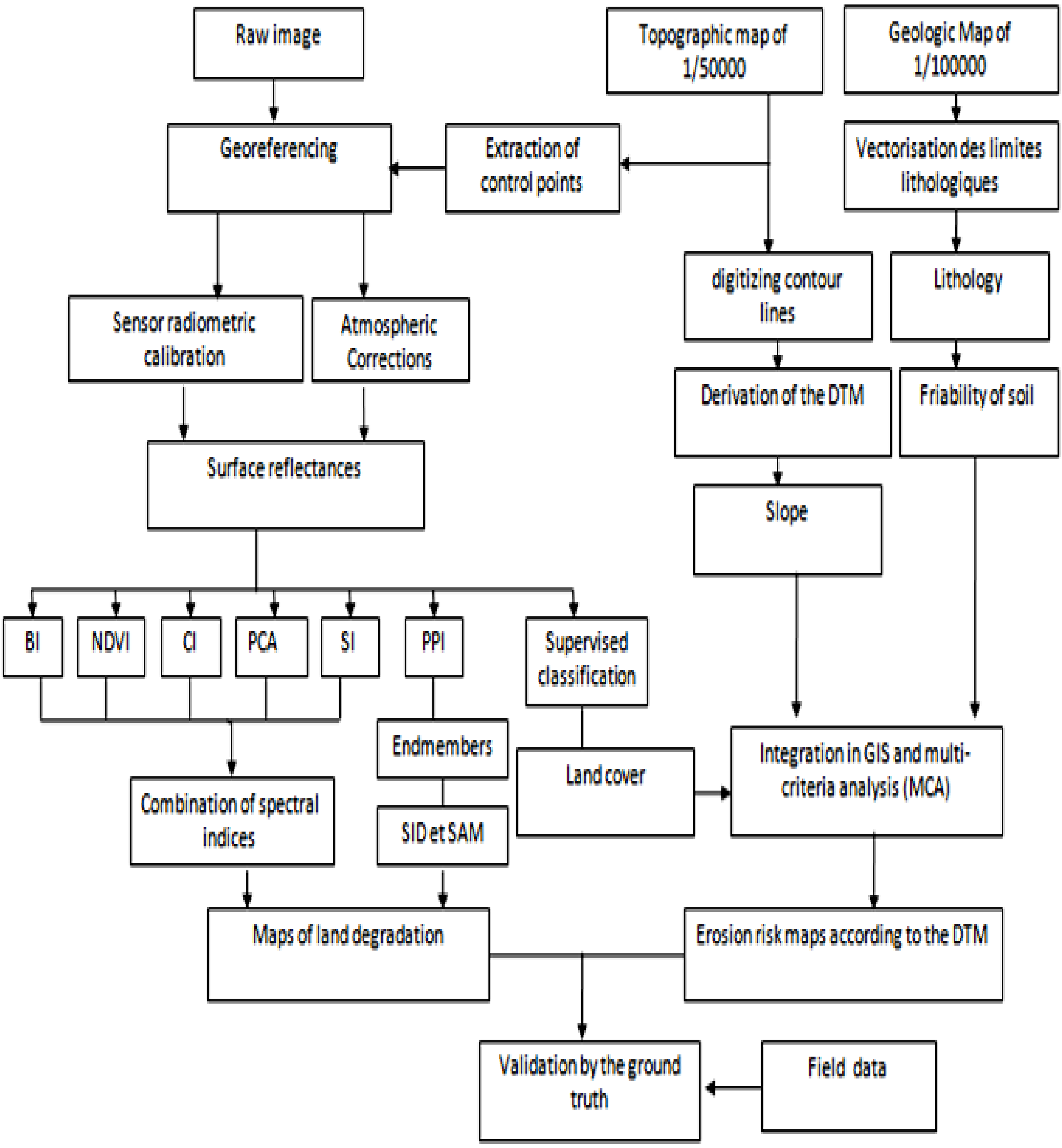

Figure 2: Methodology flowchart

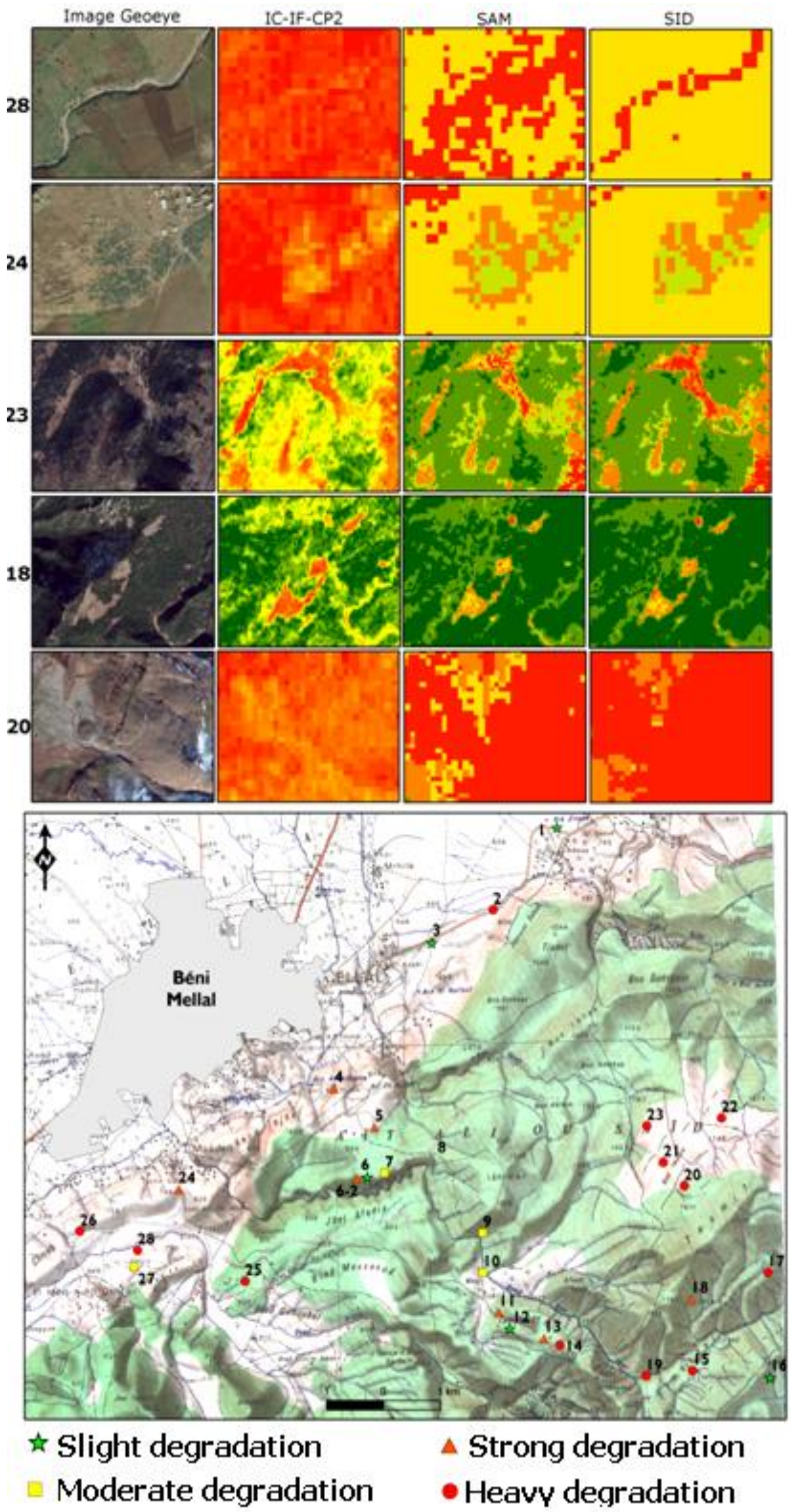

Figure 9: Validation of produced maps by the spectral indices, SAM and SID classifications by Geo-Eye imaging and field observations.